

The structure of the sedimentary cover and crystalline crust in the Sichuan Basin and its tectonic implications

Zigen Wei,^{1,2} Risheng Chu^{1,2}, Ling Chen^{1,2,3,4}, Shanshan Wu,⁵ Hui Jiang⁶ and Bin He⁷

¹State Key Laboratory of Geodesy and Earth's Dynamics, Innovation Academy for Precision Measurement Science and Technology, Chinese Academy of Sciences, Wuhan 430077, China. E-mail: chur@apm.ac.cn

²University of Chinese Academy of Sciences, Beijing 100049, China

³State Key Laboratory of Lithospheric Evolution, Institute of Geology and Geophysics, Chinese Academy of Sciences, Beijing 100029, China

⁴CAS Center for Excellence in Tibetan Plateau Earth Sciences, Beijing 100101, China

⁵Shanghai Earthquake Agency, Shanghai 200062, China

⁶Institute of Geophysics, China Earthquake Administration, Beijing 100081, China

⁷Jiangsu Earthquake Agency, Nanjing 210014, China

Accepted 2020 September 1. Received 2020 August 20; in original form 2020 March 11

SUMMARY

The Sichuan Basin, located to the east of the Tibetan Plateau, experienced successive marine and continental depositions since the Sinian. Structures of the sedimentary cover and crystalline crust, for example, thickness and V_p/V_s ratio, are of great significance to study the basin's properties and evolution, which have not been investigated simultaneously. In this paper, we extended the traditional single-layer $H-k$ stacking method of receiver functions to a multilayer $H-k$ stacking approach and applied it to invert for thickness and V_p/V_s ratio of the sedimentary cover and crystalline crust beneath 14 seismic stations in the Sichuan Basin. The observed thickness and V_p/V_s ratio of the sedimentary cover range from 4.2 to 7.5 km and from 1.86 to 2.55, respectively, suggesting unconsolidated sediments containing water or other fluids. Two-layer sedimentary cover was observed beneath eight stations, probably corresponding to the sediment in the Phanerozoic and Precambrian. The observed thickness and V_p/V_s ratio of the crystalline crust range from 33.4 to 41.8 km and from 1.61 to 1.78, respectively, suggesting typical cratonic crust in the Sichuan Basin. Theoretical analyses of $H-k$ stacking were further performed for different types of sedimentary basins, and the results suggest that the multilayer $H-k$ stacking is more effective to study basin's structure with a thick sedimentary layer and thin subsediment crust.

Key words: Composition and structure of the continental crust; Asia; Body waves; Crustal imaging; Cratons.

1 INTRODUCTION

The sedimentary cover keeps a record of formation and evolution of a basin, which usually hosts petroleum and mineral deposits. The low-velocity sedimentary cover introduces error and false image beneath the subsediment crust, such as the crustal thickness and S -wave velocity, in traditional receiver-function (RF) analysis methods due to the complex and strong reverberation from the sedimentary package (Aki & Richards 1980; Yeck *et al.* 2013; Zhang & Gao 2019). The low-velocity sedimentary layer also amplifies the amplitude of seismic waves and imposes larger seismic hazards (Aki & Richards 1980; Yu & Haines 2003; Deng 2013). In addition, the properties and stress states of crustal bedrock beneath the sedimentary layer are closely related to the tectonic evolution and dynamic background of the deep crust. Therefore, the structural characteristics of the sedimentary layer and underlying bedrock of

the basin provide valuable information for fossil fuel exploration and earthquake mitigation and can be used to accurately image the deep crust and mantle.

The Sichuan Basin (Fig. 1), located in the transtensional tectonic region between the Tethyan–Himalayan and the Pacific tectonic domains, is an ancient cratonic intracontinental basin (Deng 2013). The Sichuan Basin has undergone multiple extensional and compressional tectonic events (Molnar & Tapponnier 1975), and mainly experienced marine deposition in the Sinian–Late Triassic, continental deposition in the Late Triassic–Late Cretaceous and differential uplift since the Late Cretaceous (Liu *et al.* 2011). The long-term sedimentary history and complex tectonic evolution of the Sichuan Basin have led to the formation of abundant fossil fuel and mineral resources. Compared with rare strong earthquakes occurred in the interior, the western edge of the Sichuan Basin is prone to destructive earthquakes (Fig. 1), such as the 2008 M_s 8.0 Wenchuan

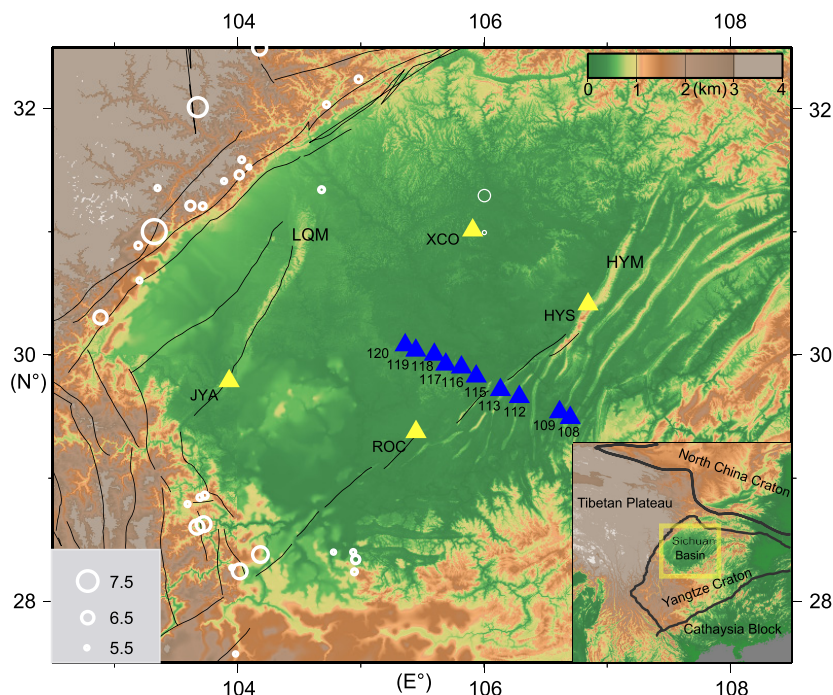


Figure 1. Map showing the topography, tectonic setting (right inset), seismic stations (triangles) and earthquakes (white circles) with magnitudes > 5.5 occurring from 1500 AD to 2019 in the Sichuan Basin and its surroundings. LQM: Longquan Mountains; HYM: Huaying Mountains.

earthquake, which caused huge casualties and property losses. The abundant fossil fuel and mineral resources and the special distribution of strong earthquakes in the Sichuan Basin make the study of its sedimentary cover and crystalline crust interesting and significant.

Numerous geological and geophysical studies have been carried out in the Sichuan Basin. The Archean-early Proterozoic crystalline basement in the Sichuan Basin is separated by an unconformity from overlying middle Neoproterozoic metamorphic strata and late Neoproterozoic unmetamorphosed strata (Zhao & Cawood 2012). Rocks with ages of 2.9–2.95 Ga are exposed along its western edge (Greentree & Li 2008), whereas, in general, most exposed sediments are Jurassic-Cretaceous in age (Deng 2013). Seismic studies have imaged a crustal thickness of 40–45 km with normal velocity, an increasing sediment thickness from east to west and a high-velocity lithosphere with a thickness of ~ 200 km through seismic explorations (Wang *et al.* 2016, 2017; Zhang *et al.* 2019), RF imaging (Liu *et al.* 2014; Wei *et al.* 2017; Zhang *et al.* 2018), surface wave tomography (Li *et al.* 2009; Zheng *et al.* 2010) and body-wave tomography (Zhao *et al.* 2013).

Thickness and V_p/V_s ratio of the sedimentary and bedrock layers in the crust are closely related to rock composition, crustal stress state and tectonic evolution (Christensen 1996; Ji *et al.* 2009). The H - k stacking method of RFs (Zhu & Kanamori 2000) has been widely used to invert the crustal thickness and average V_p/V_s ratio by joint analysis of major seismic phases from the Moho in recent years (He *et al.* 2014; Wang *et al.* 2014; Wei *et al.* 2016a; Guo *et al.* 2019). However, the results from this method usually deviate from the true values when a thick sedimentary layer exists in the crust (Yeck *et al.* 2013; Wei *et al.* 2016b). The sequential H - k stacking method (Yeck *et al.* 2013) and autocorrelation-filter H - k stacking method (Yu *et al.* 2015) for RFs were developed to obtain the thickness and V_p/V_s ratio of the single-layer sedimentary layer and subsediment crust. Although some seismic studies have been carried out (Li *et al.* 2009, 2014; Wang *et al.* 2016), the thickness

and V_p/V_s ratio of the sedimentary cover and crystalline crust have not been simultaneously investigated in the Sichuan Basin. In this study, we first expand the sequential H - k stacking method for RFs (Yeck *et al.* 2013) from two layers to multiple layers in the crust and then use the multilayer H - k stacking method to invert the thickness and average V_p/V_s ratio of the sedimentary layers and subsediment crust for 14 seismic stations in the Sichuan Basin. The structural characteristics are further used to analyse the tectonic implications for the Sichuan Basin.

2 DATA AND METHOD

2.1 Data

Teleseismic RFs are used to invert the crustal structure in the Sichuan Basin. Teleseismic waveforms from 10 temporary stations (blue triangles in Fig. 1) with 10–20 km station spacing are collected from the Seismic Array Laboratory, Institute of Geology and Geophysics, Chinese Academy of Sciences (Wang *et al.* 2018; Zhang *et al.* 2018). These stations are all equipped with Guralp CMG-3ESP sensors (0.02–30 s) and were operated for 12 to 18 months from 2000 to 2012. Teleseismic data recorded from 2007 July to 2010 May from four permanent stations (yellow triangles) were obtained from the Data Management Center of China National Seismic Network through Institute of Geophysics, China Earthquake Administration (doi:10.11998/SeisDmc/SN, <http://www.seis-dmc.ac.cn>, Zheng *et al.* 2010). These stations are equipped with Guralp CMG-3ESP sensors with a bandwidth of 0.02–60 s. Earthquake data with > 5.5 magnitudes, 30° – 90° epicentral distances and 30° – 210° backazimuths where most events fall in, were used to further extract the RFs (Fig. 2).

We trimmed the teleseismic data from 20 s before to 100 s after the direct P -wave arrivals and then calculated the radial RFs using a high Gaussian factor of 5.0 and a lower Gaussian factor of 2.0 and water

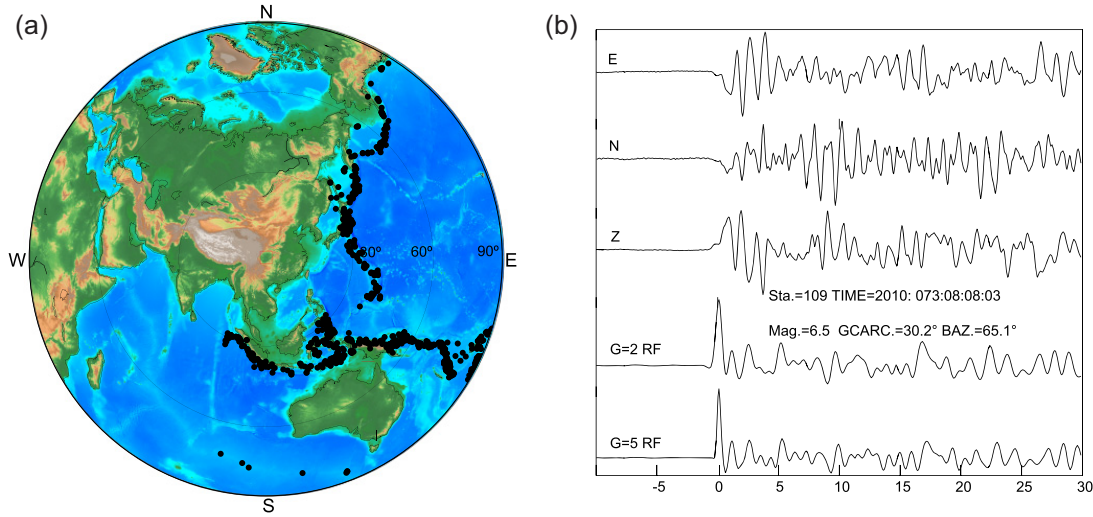


Figure 2. (a) Teleseismic event distribution (solid dots) used for all stations referred to the location (105.5°E, 30.0°N) in the study region (red rectangle). (b) shows the teleseismic waveforms of horizontal (E, N) and vertical (Z) components and corresponding radial RFs with Gaussian factor of 5.0 and 2.0 for an event recorded by station 109.

level of 0.01 by a time-domain maximum entropy deconvolution method (Wu & Zeng 1998). For these data, we removed RFs with indistinguishable Ps arrivals by visual inspection and kept 1895 high-quality RFs for further analysis. The selected RFs were then subjected to moveout correction for both the Ps and PpPs arrival times of the Moho based on a ray parameter of 0.065 s km^{-1} (Liu & Niu 2012). The stacked RFs with different Gaussian factors of 2.0 and 5.0 are shown for each station in Fig. 3.

2.2 Methods

2.2.1 Single-layer H - k stacking method

The time differences between different phases from the discontinuities in RFs can be used to obtain deep structural information. The single-layer H - k stacking method of RFs (Zhu & Kanamori 2000) was developed to study the crustal thickness (H) and average V_p/V_s ratio (k) simultaneously utilizing the converted Ps and multiple PpPs/PpSs + PsPs phases from the Moho. In this method, the maximum stacking amplitude of $S(H, k)$ corresponds to the optimal H and k in an H - k domain (1):

$$S(H, k) = w_{Ps}r(t_{Ps}) + w_{PpPs}r(t_{PpPs}) - w_{PpSs+PsPs}r(t_{PpSs}). \quad (1)$$

In eq. (1), $r(t)$ represents the RFs and w_{Ps} , w_{PpPs} and $w_{PpSs+PsPs}$ are weighting factors with summation of 1. Additionally, t_{Ps} , t_{PpPs} and $t_{PpSs+PsPs}$ are the predicted arrival times of the phases. This method can avoid the human error involved in manually picking arrival times of different phases from the Moho and is widely used to study crustal thickness and average V_p/V_s ratio beneath seismic stations (He *et al.* 2014; Wang *et al.* 2014; Wei *et al.* 2016a).

2.2.2 Sequential multilayer H - k stacking method

Seismic discontinuities in crust can reflect P or S phases and can convert P phases to S phases. Therefore, the converted Ps and multiple PpPs/PpSs + PsPs phases from discontinuities, such as the sediment/bedrock interface and intrasedimentary interfaces, will also be received by the seismometer. Yeck *et al.* (2013) extended the single-layer H - k stacking method (Zhu & Kanamori 2000) to

an iterative two-layer H - k stacking approach. In the approach, a single-layer H - k stack with high-frequency RFs is first performed to obtain the sedimentary thickness and average V_p/V_s ratio. Then, a modified single-layer H - k stack with lower-frequency RFs is performed to constrain subsediment crustal properties using the basin results as a priori information. We extend the two-layer H - k stacking approach to multilayer H - k stacking using a similar concept. High-frequency and lower-frequency RFs are used to study the sediment and basement crustal properties:

$$t_{Ps} = \sum_i h_i \times \left(\sqrt{k_i^2/v_{pi}^2 - p^2} - \sqrt{1/v_{pi}^2 - p^2} \right) \quad (2)$$

$$t_{PpPs} = \sum_i h_i \times \left(\sqrt{k_i^2/v_{pi}^2 - p^2} + \sqrt{1/v_{pi}^2 - p^2} \right) \quad (3)$$

$$t_{PpSs+PsPs} = \sum_i 2 \times h_i \times \sqrt{k_i^2/v_{pi}^2 - p^2}, \quad (4)$$

where i is the number of layers in the crust; k_i , V_{pi} and h_i are the V_p/V_s ratio, P -velocity and thickness for the i th layer, respectively; p is the ray parameter; and t_{Ps} , t_{PpPs} and $t_{PpSs+PsPs}$ are the predicted arrival times of the phases. As an example, for a three-layer crust containing two sediment layer, we first calculate the upper-layer ($i = 1$) properties with the single-layer H - k stacking method using high-frequency RFs, then estimate the middle-layer ($i = 2$) properties by a modified H - k stack using upper-layer results as *a priori* information and finally calculate the lower-layer ($i = 3$) properties by a modified H - k stack using the upper-layer and middle-layer results as *a priori* information.

Synthetic RFs with 0 km thick sediment, 6 km thick single-layer sediment and 8 km thick two-layer sediment are calculated with different Gaussian factors of 2.0 and 5.0 (Fig. 4). In these models, the crust is set to 40 km thick, and the velocities of the sediment and basement crust are from seismic exploration results (Wang *et al.* 2016, 2017) and the global AK135 model (Kennett *et al.* 1995), respectively. The phases from the sediment/bedrock interface are clear in the RFs with a Gaussian factor of 5 but unrecognizable in the RFs with a Gaussian factor of 2. The arrival times of the Ps and

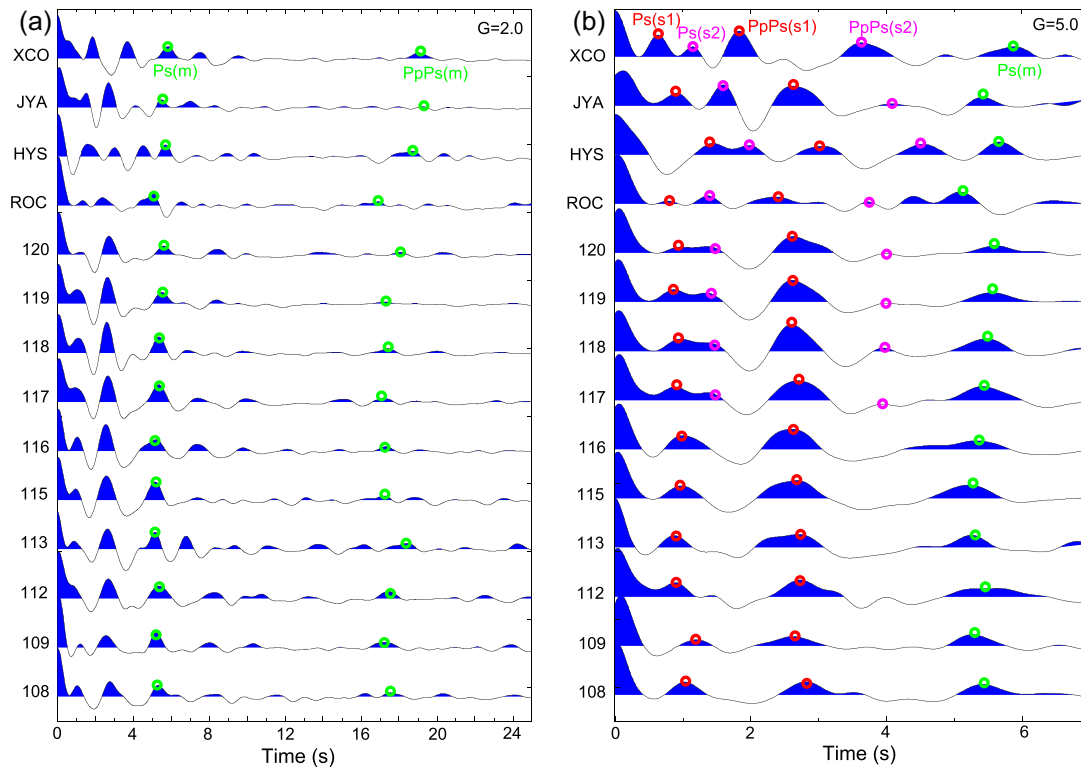


Figure 3. Stacked RFs from all backazimuths for each station with different Gaussian factors (G). Green circles show the theoretical arrival times for the main phases from the Moho (m). Red and pink circles mark the theoretical arrival times for the main phases from the base of the upper sediment layer (s1) and the lower sediment layer (s2), respectively.

PpPs phases associated with basement phases are earlier than the Ps phases associated with the Moho.

Clear Ps and PpPs phases associated with the sediment are observed at all the stations (Fig. 3b), and the results are comparable to the synthetic RFs (Fig. 4). For the stations 108, 109, 112, 113, 115 and 116, we used the two-layer H - k stacking approach to calculate the thicknesses and V_p/V_s ratios of the sedimentary cover and subsediment crust based on the waveform characteristic for these stations. The P velocities for the first and second layers are set to 5.5 and 6.6 km s⁻¹, respectively, based on seismic exploration data (Wang *et al.* 2016). For other stations, we applied the three-layer H - k stacking method to estimate the properties of the sedimentary layer and subsediment crust. The P velocities for the first, second and third layers are set to 5.0, 6.0 and 6.6 km s⁻¹, respectively (Wang *et al.* 2016). The weights are set to 0.5, 0.5 and 0.0 for the Ps, PpPs and PsPs + PsPs phases, respectively, based on their progressive decrease in the signal-to-noise ratio. Figs 5 and 6 show the RF and sequential two-layer and three-layer H - k stacking result for typical stations, respectively.

3 RESULTS

Table 1 shows the thicknesses and V_p/V_s ratios of the sedimentary cover and subsediment crust for each station in the study region using the sequential H - k stacking method. For the sedimentary cover, the thickness and average V_p/V_s ratio range from 4.2 to 7.5 km and 1.86 to 2.55, respectively. For the subsediment crust, the thickness and V_p/V_s ratio range from 33.4 to 41.8 km and 1.61 to 1.78, respectively. Thus, the crustal thickness and average V_p/V_s ratio range from 40.9 to 47.9 km and 1.67 to 1.80, respectively.

4 DISCUSSION

4.1 Crustal structure in the Sichuan Basin

4.1.1 Feasibility analysis for two-layer sedimentary cover in the Sichuan Basin

Geological observations reveal that the Sichuan Basin experienced marine and continental deposition in succession since the Sinian (Liu *et al.* 2011; Deng 2013). For stations ROC, HYS, JYA and XCO, clear Ps and PpPs phases are observed from the upper sediment layer and the lower sediment layer (Fig. 3b), suggesting a two-layer sedimentary cover. For stations 117–120, strong and weak energy exists at approximately 1.4 and 4.0 s, respectively (Fig. 3b), which is probably to be associated with the lower sediment layer with a small impedance contrast. For these stations, the thickness of the sedimentary layer varies from 6.7 to 7.5 km by a three-layer H - k stacking, which is close to the seismic exploration results (Wang *et al.* 2016, 2017). The observed two-layer sediments beneath these stations may reflect the true structure of the sedimentary cover, which may correspond to the sediment in the Phanerozoic and Precambrian (Deng 2013; Wang *et al.* 2017), respectively.

4.1.2 Structure of sedimentary cover in the Sichuan Basin

The observed thickness and V_p/V_s ratio of the sedimentary cover varied from 4.2 to 7.5 km and 1.86 to 2.55 in the study region, respectively (Table 1, Fig. 7). The thickness of the sedimentary layer is generally 2–3 km thinner than the thickness estimated from seismic exploration (Wang *et al.* 2016, 2017) and geological data (Deng 2013) on the Phanerozoic and Precambrian deposits in the

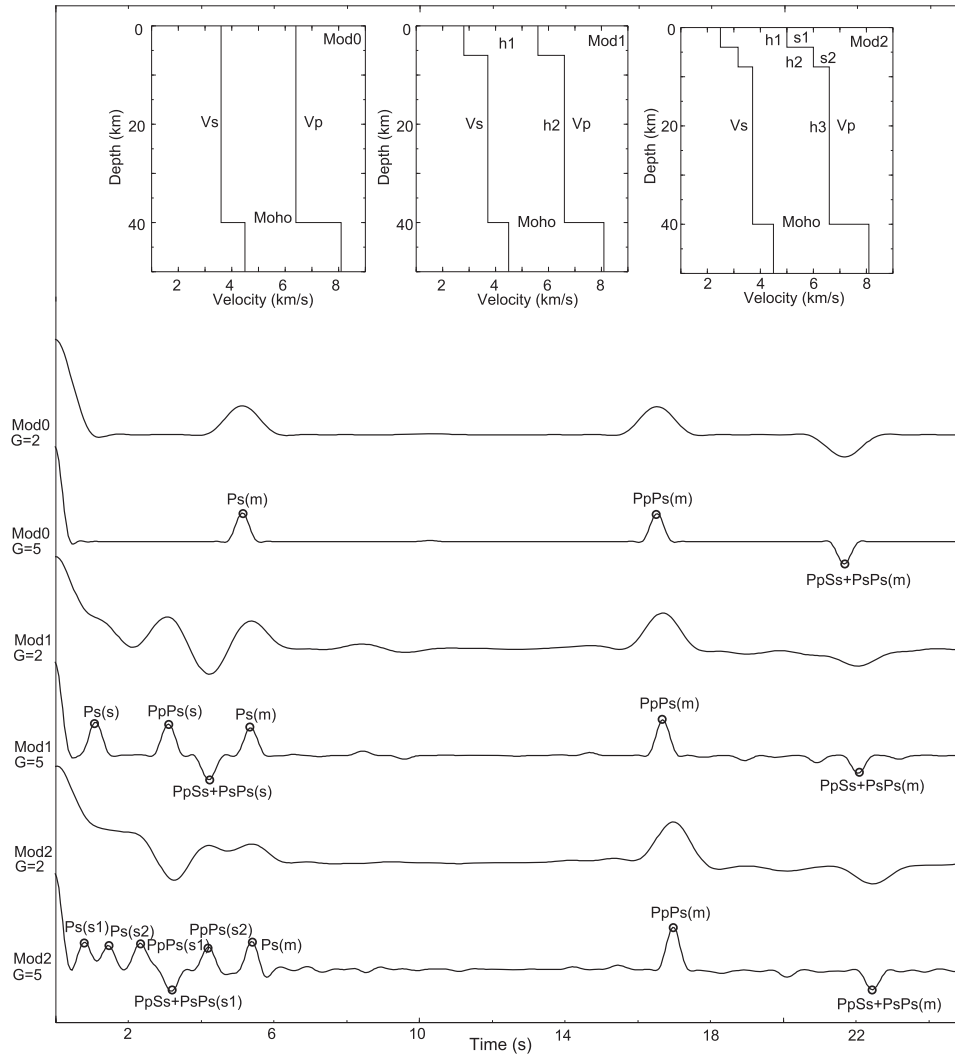


Figure 4. Synthetic RFs with different Gaussian values (G) of 2.0 and 5.0 from different velocity models (Mod) containing one- or two-layer sediment (s1, s2). Circles mark the main phases from the Moho (m) and the base of the sedimentary package.

basin. The observed sedimentary cover for the stations 108, 109, 112, 113, 115 and 116 may exclusively reflect the Precambrian deposits, whose bottom impedance contrast associated with gravitational compaction is probably too small to generate RF phases. The V_p/V_s ratio of the sedimentary layer is significantly higher than that of the crystalline crust, with a maximum value of 2.55 at station 109. High V_p/V_s ratios in sedimentary cover are also found in the Powder River Basin and the Denver Basin in the United States (Yeck *et al.* 2013) and the Songliao Basin in China (Yu *et al.* 2015). In general, unconsolidated sediments and cataclasites related to faults that are saturated with water or other fluids exist in the sedimentary cover (Ji *et al.* 2009), and these conditions can significantly increase the V_p/V_s ratio in the study region.

4.1.3 Structure of the crystalline crust in the Sichuan Basin

The V_p/V_s ratio of the crystalline crust ranges from 1.64 and 1.78 (Table 1, Fig. 7), suggesting that partial melting or intrusion of mafic material has not yet occurred in the study region, as these processes can significantly increase the V_p/V_s ratio to > 1.87 (Ji *et al.* 2009). The average values of crustal thickness and V_p/V_s ratio

are 43.7 km and 1.74, respectively, which are comparable to the characteristics of Precambrian shields (Zandt & Ammon 1995). The observed low V_p/V_s ratio of the crystalline crust, together with the high-velocity and well-defined stratification of the crustal velocity (Li *et al.* 2009), ~ 200 km thick lithosphere (Zhao *et al.* 2013), suggests that the Sichuan Basin still maintains the characteristics of a typical craton and preserves a rigid crust. The rigid crust is consistent with the rare medium-strong earthquake occurred in the interior of the Sichuan Basin, suggests the inexistence of large-scale active faults with fluid. In contrast, the western edge of the Sichuan Basin has been affected by the compression from the uplift of the Tibetan Plateau, which leads to the formation of large faults and the occurrence of destructive earthquakes (Fig. 1).

4.2 Comparison between the single-layer and multilayer $H-k$ stacking methods

We estimated the crustal average P -wave velocity (\bar{V}_p) for each station in the study region based on the above multilayer $H-k$ stacking results (Table 1). Then, we recalculated the crustal thickness and average k for these stations using the single-layer $H-k$ stacking

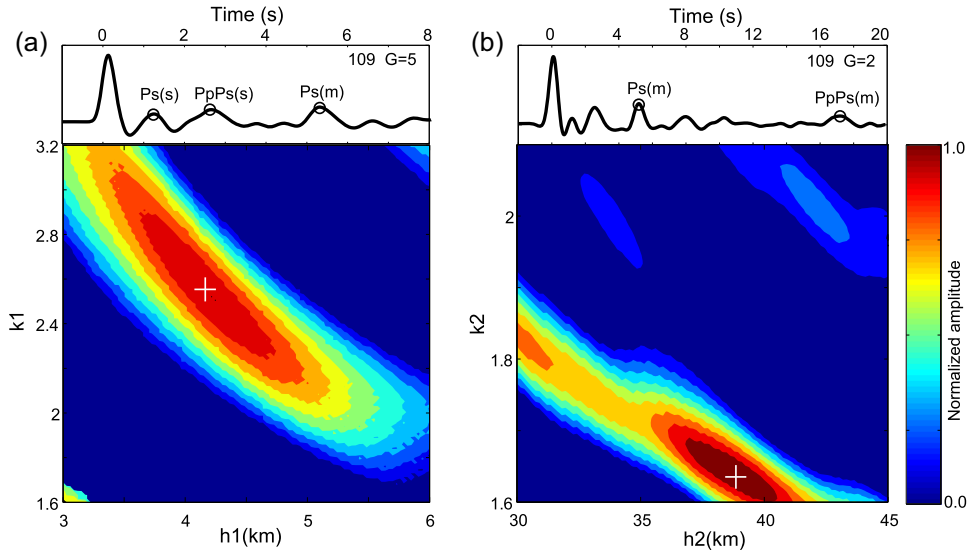


Figure 5. The RF and sequential H - k stacking results for crust with one-layer sediment (s) for the station 109. h_1 and h_2 represent the thicknesses of the sediment layer and layer from the bottom of the sediment to the Moho (m), respectively. k_1 and k_2 represent the average V_p/V_s ratios in h_1 and h_2 , respectively. The optimal thickness and average V_p/V_s ratio are shown in the crosses. G represents the Gaussian factor.

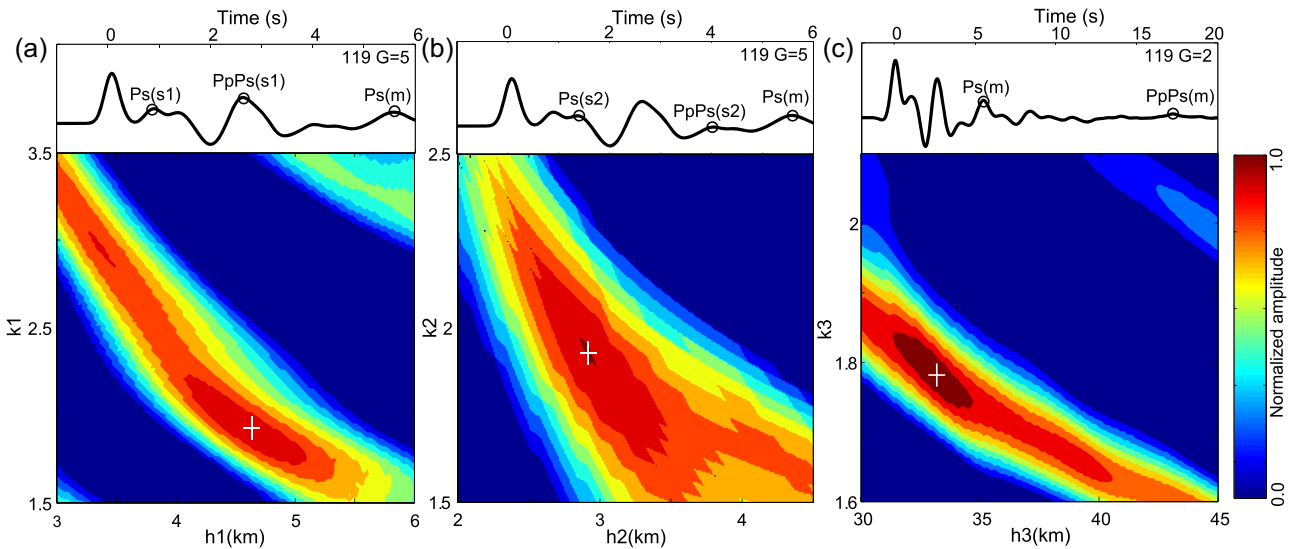


Figure 6. The RF and sequential H - k stacking results for crust with two-layer sediment for the station 119. h_1 , h_2 and h_3 represent the thicknesses of the upper sediment layer (s1), the lower sediment layer (s2) and the layer from the base of the sediment to the Moho (m), respectively. k_1 , k_2 and k_3 represent the V_p/V_s ratios of h_1 , h_2 and h_3 , respectively. The optimal thicknesses and V_p/V_s ratios are shown in the crosses. G represents the Gaussian factor.

method given the above $\overline{V_p}$ values. The results show that the crustal thicknesses calculated by single-layer and two-layer H - k stacking are almost the same. The k values from the single-layer H - k stacking are mostly less than 1.77 and are generally 1–3 per cent higher than those of the crystalline crust from the multilayer H - k stacking. Therefore, we conclude that typical cratonic crust is preserved in the study region from the single-layer H - k stacking results, which is consistent with previous H - k stacking results (He *et al.* 2014; Wei *et al.* 2016a).

Multiple crustal models containing one-layer sediment (h_1 , k_1) and one-layer crystalline crust (h_2 , k_2) were further theoretically analysed using the single-layer H - k stacking method (Table 2). In these models, the P -wave velocities and average V_p/V_s ratios in the sediment and crystalline crust were set to 5.5 and 6.6 km s⁻¹ and 2.0

and 1.76, respectively. The differences in both H and k between the single-layer H - k stacking results and the true values are less than 1 per cent for all models when the thickness of the sediment is 2 km. For the models with 6 km thick sediment, the differences in both H and k between the single-layer H - k stacking results and the true values increase with the thinning of crystalline crust. The k value of the single-layer H - k stacking reaches 1.86 with 6 km thick sediment and 30 km thick crystalline crust, which is easily misinterpreted as being related to partial melting or the intrusion of mafic material in the crystalline crust. For the model with 6 km thick sediment and 26 km thick crystalline crust, the differences in H and k between the single-layer H - k stacking results and the true values are close to 11 and 18 per cent, respectively. The reason is that the PpPs phase of the sediment is identified as the Ps phase of the Moho by the single-layer

Table 1. Thicknesses and V_p/V_s ratios of different layers in crust for each station. h_1 , h_2 and h_3 represent the thicknesses (km) of the upper sediment layer, the lower sediment layer and the layer from the base of the sediment to the Moho, respectively. k_1 , k_2 and k_3 represent the V_p/V_s ratios of h_1 , h_2 and h_3 , respectively. H and $Av.k$ represent the crustal thickness (km) and average V_p/V_s ratio for the stations. Sta., Lon. and Lat. represent the name, longitude and latitude of the seismic stations, respectively.

Sta.	Lon.	Lat.	h_1	k_1	h_2	k_2	h_3	k_3	H	$Av.k$
108	106.7	29.5	5.3	2.05			38.0	1.70	43.3	1.74
109	106.6	29.5	4.2	2.55			38.9	1.64	43.1	1.73
112	106.3	29.7	5.4	1.89			37.4	1.74	42.8	1.76
113	106.1	29.7	5.4	1.87			41.8	1.64	47.2	1.67
115	105.9	29.8	5.0	2.04			37.9	1.69	42.9	1.73
116	105.8	29.9	4.7	2.13			38.3	1.68	43.0	1.73
117	105.7	29.9	4.8	1.89	2.4	2.13	34.2	1.72	41.4	1.76
118	105.6	30.0	4.2	2.13	3.1	1.75	34.7	1.71	42.0	1.76
119	105.5	30.0	4.6	1.92	2.9	1.91	33.4	1.78	40.9	1.80
120	105.4	30.1	4.3	2.05	3.2	1.78	35.8	1.74	43.3	1.77
ROC	105.4	29.4	4.2	1.91	2.5	2.28	34.8	1.67	41.5	1.73
HYS	106.8	30.4	4.3	2.63	3.1	2.05	38.0	1.63	45.4	1.75
JYA	103.9	29.8	4.4	2.01	2.7	2.45	40.8	1.61	47.9	1.69
XCO	105.9	31.0	3.2	1.98	4.0	1.76	39.3	1.75	46.5	1.77

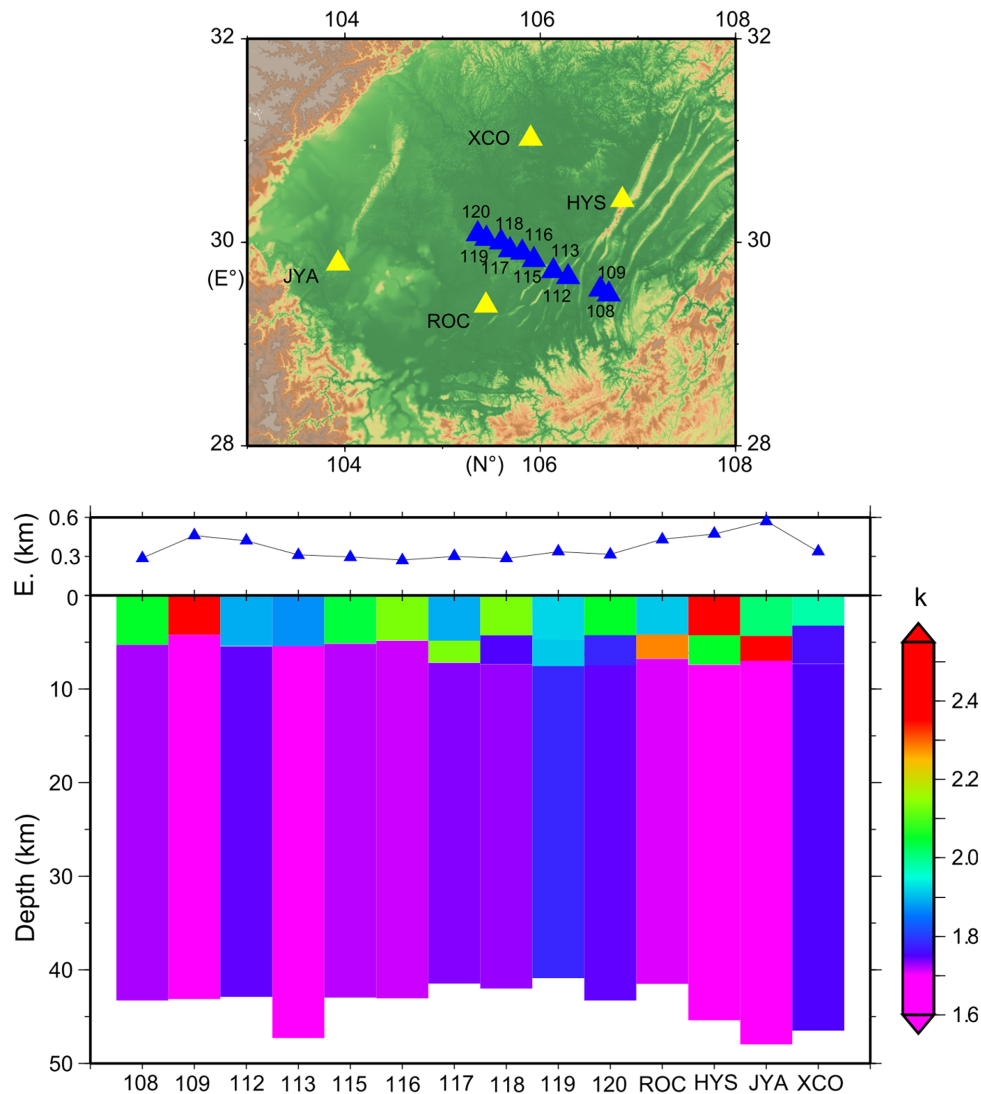


Figure 7. Thickness and V_p/V_s ratio (k) for different layers in crust beneath the seismic stations (blue triangles) in the study region. The upper panel shows the station locations (triangles). E.: Elevation.

Table 2. Theoretical tests for different crustal models using the single-layer H - k stacking method. The six models contain one-layer sediment ($h1$, $k1$) and one-layer crystalline crust ($h2$, $k2$). H and k are the crustal thickness and average V_p/V_s ratio from the single-layer H - k stacking. $\Delta h = 1 - \frac{h1+h2}{H}$; $\Delta k = 1 - \frac{k1 \times h1 + k2 \times h2}{k(h1+h2)}$.

Model	$h1$ (km)	$k1$	$h2$ (km)	$k2$	H (km)	k	Δh (%)	Δk (%)
Model1	2	2.0	38	1.76	39.6998	1.7877	-0.76	0.88
Model2	2	2.0	32	1.76	33.6730	1.7896	-0.97	0.87
Model3	2	2.0	26	1.76	27.7904	1.7904	-0.75	0.74
Model4	6	2.0	34	1.76	39.8753	1.8110	-0.31	0.83
Model5	6	2.0	30	1.76	35.209	1.8601	-2.25	3.23
Model6	6	2.0	26	1.76	35.9291	1.5288	10.94	-18.07

H - k stacking method due to the overlap of the positive Ps phase of the Moho and the negative PsPs/PpSs phase of the sediment. The above theoretical tests suggest that the single-layer H - k stacking method is not suitable for the study of crustal structure in regions with thick sedimentary cover and thin crystalline crust, such as the Songliao Basin in NE China. The multilayer H - k stacking method is required to study the thickness and V_p/V_s ratio of sedimentary and crystalline crust in this region.

5 CONCLUSIONS

In this paper, we extended the traditional H - k stacking method of RFs to the multilayer H - k stacking and then applied the new approach to obtain the thickness and V_p/V_s ratio of sedimentary cover and subsediment crust beneath 14 stations in the Sichuan Basin. The observed thicknesses of the sedimentary cover and subsediment crust vary from 4.2 to 7.5 km and from 33.4 to 41.8 km, respectively. The observed V_p/V_s ratios of the sedimentary cover and subsediment crust range from 1.86 to 2.55 and from 1.61 to 1.78, respectively. The high V_p/V_s ratio in the sedimentary cover may be related to unconsolidated sediments containing water or other fluids, which may mainly consist of Phanerozoic deposits. The observed low V_p/V_s ratios and normal thickness of the crystalline crust suggest the presence of typical cratonic crust in the Sichuan Basin. In addition, we theoretically analysed and compared the applicability of single-layer and multilayer H - k stacking methods for different types of sedimentary basins. The results of the single-layer and multilayer H - k stacking methods in the Sichuan Basin are comparable. However, the single-layer H - k stacking method is not suitable for the study of crustal structure in regions with thick sedimentary layers and thin subsediment crust, such as the Songliao Basin in NE China.

ACKNOWLEDGEMENTS

We are thankful to the Seismic Array Laboratory, Institute of Geology and Geophysics, Chinese Academy of Sciences (doi:10.12129/IGGSL.Data.Observation, <http://www.seislab.cn/>) and Data Management Centre of China National Seismic Network at Institute of Geophysics (SEISDMC, doi:10.11998/SeisDmc/SN), China Earthquake Administration, for providing seismic data of temporary and permanent stations, respectively. We thank the Editor and two anonymous reviewers for their constructive reviews. This work is supported by the DREAM project of the National Key Research and Development Program of China (Grant No. 2016YFC0600402) and the National Natural Science Foundation of China (Grant No. 41604056).

REFERENCES

- Aki, K. & Richards, P.G., 1980. *Quantitative Seismology: Theory and Methods*, W. H. Freeman and Company.
- Christensen, N.I., 1996. Poisson's ratio and crustal seismology, *J. geophys. Res.*, **101**, 3139–3156.
- Deng, B., 2013. Meso-Cenozoic architecture of basin-mountain system in the Sichuan basin and its gas distribution, *PhD thesis*, Chengdu University of Technology, Chengdu (in Chinese with English abstract).
- Greentree, M.R. & Li, Z.X., 2008. The oldest known rocks in south-western China, SHRIMP U-Pb magmatic crystallisation age and detrital provenance analysis of the Paleoproterozoic Dahongshan Group, *J. Asian Earth Sci.*, **33**(5), 289–302.
- Guo, L.H., Gao, R., Shi, L., Huang, Z. & Ma, Y.W., 2019. Crustal thickness and Poisson's ratios of south china revealed from joint inversion of receiver function and gravity data, *Earth planet. Sci. Lett.*, **510**, 142–152.
- He, R.Z., Shang, X.F., Yu, C.Q., Zhang, H.J. & van der Hilst, R., 2014. A unified map of Moho depth and V_p/V_s ratio of continental China by receiver function analysis, *Geophys. J. Int.*, **199**, 1910–1918.
- Ji, S.C., Wang, Q. & Salisbury, M.H., 2009. Composition and tectonic evolution of the Chinese continental crust constrained by Poisson's ratio, *Tectonophysics*, **463**, 15–30.
- Kennett, B.L.N., Engdahl, E.R. & Buland, R., 1995. Constraints on seismic velocities in the Earth from traveltimes, *Geophys. J. Int.*, **122**(1), 108–124.
- Li, H.Y., Su, W., Wang, C.Y. & Huang, Z.X., 2009. Ambient noise Rayleigh wave tomography in western Sichuan and eastern Tibet, *Earth planet. Sci. Lett.*, **282**, 201–211.
- Li, Y.H., Gao, M.T. & Wu, Q.J., 2014. Crustal thickness map of the Chinese mainland from teleseismic receiver functions, *Tectonophysics*, **611**, 51–60.
- Liu, H.F. & Niu, F.L., 2012. Estimating crustal seismic anisotropy with a joint analysis of radial and transverse receiver function data, *Geophys. J. Int.*, **188**(1), 144–164.
- Liu, Q.Y. et al., 2014. Eastward expansion of the Tibetan Plateau by crustal flow and strain partitioning across faults, *Nat. Geosci.*, **7**(5), 361–365.
- Liu, S.G., Deng, B., Li, Z.W. & Sun, W., 2011. The texture of sedimentary basin-orogenic belt system and its influence on oil/gas distribution: a case study from Sichuan basin, *Acta Petrol. Sin.*, **27**(3), 621–635, (in Chinese with English abstract).
- Molnar, P. & Tapponnier, P., 1975. Cenozoic tectonics of Asia: effects of a continental collision, *Science*, **189**, 419–426.
- Wang, C.Y., Sandvol, E., Zhu, L.P., Lou, H., Yao, Z.X. & Luo, X.H., 2014. Lateral variation of crustal structure in the Ordos block and surrounding regions, North China, and its tectonic implications, *Earth planet. Sci. Lett.*, **387**, 198–211.
- Wang, H.Y. et al., 2017. Deep crustal structure in Sichuan basin: deep seismic reflection profiling, *Chin. J. Geophys.*, **60**(8), 2913–2923, (in Chinese with English abstract).
- Wang, M.M., Hubbard, J., Plesch, A., Shaw, J.H. & Wang, L.M., 2016. Three-dimensional seismic velocity structure in the Sichuan basin, China, *J. geophys. Res.*, **121**(2), 1007–1022.
- Wang, X., Cheng, L., Ai, Y.S., Xu, T., Jiang, M.M., Ling, Y. & Gao, Y.F., 2018. Crustal structure and deformation beneath eastern and northeastern Tibet revealed by P -wave receiver functions, *Earth planet. Sci. Lett.*, **497**, 69–79.

- Wei, Z.G., Chen, L., Li, Z.W., Ling, Y. & Li, J., 2016a. Regional variation in Moho depth and Poisson's ratio beneath eastern China and its tectonic implications, *J. Asian Earth Sci.*, **115**, 308–320.
- Wei, Z.G., Chu, R.S., Chen, L., Chong, J.J. & Li, Z.W., 2016b. Analysis of $H-k$ stacking of receiver functions beneath crust with complex structure: taking the Anatolia plate as an example, *Chin. J. Geophys.*, **59**(11), 4048–4062, (in Chinese with English abstract).
- Wei, Z.G., Chu, R.S., Li, Z.W., Sheng, M.H., Zhang, H.J. & Wang, B.S., 2017. Structures of Xishan village landslide in Li County, Sichuan, inferred from high-frequency receiver functions of local earthquakes, *Chin. J. Geophys.*, **60**(10), 3793–3803, (in Chinese with English abstract).
- Wu, Q.J. & Zeng, R.S., 1998. The crustal structure of Qinghai-Xizang plateau inferred from broadband teleseismic waveform, *Chin. J. Geophys.*, **41**(5), 669–679, (in Chinese with English abstract).
- Yeck, W.L., Sheehan, A.F. & Schulte, P.V., 2013. Sequential $H-k$ stacking to obtain accurate crustal thicknesses beneath sedimentary basins, *Bull. seism. Soc. Am.*, **103**, 2142–2150.
- Yu, J.S. & Haines, J., 2003. The choice of reference sites for seismic ground amplification analyses: case study at Parkway, New Zealand, *Bull. seism. Soc. Am.*, **93**(2), 713–723.
- Yu, Y.Q., Song, J.G., Liu, K.H. & Gao, S.S., 2015. Determining crustal structure beneath seismic stations overlying a low-velocity sedimentary layer using receiver functions, *J. geophys. Res.*, **120**, 3208–3218.
- Zandt, G. & Ammon, C.J., 1995. Continental crust composition constrained by measurements of crustal Poisson's ratio, *Nature*, **374**, 152–154.
- Zhang, J.Y., Chen, L. & Wang, X., 2019. Crustal structure study based on principal component analysis of receiver functions, *Sci. China Earth Sci.*, **62**, 1110–1124.
- Zhang, Y.Y., Chen, L., Ai, Y.S., Jiang, M.M., Xu, W.W. & Shen, Z.Y., 2018. Lithospheric structure of the South China Block from S receiver function, *Chin. J. Geophys.*, **61**(1), 138–149, (in Chinese with English abstract).
- Zhang, Z.Q. & Gao, Y., 2019. Crustal thicknesses and Poisson's ratios beneath the Chuxiong-Simao basin in the southeast margin of the Tibetan Plateau, *Earth Planet. Phys.*, **3**(1), 69–84.
- Zhao, G.C. & Cawood, P.A., 2012. Precambrian geology of China, *Precambrian Res.*, **222–223**, 13–54.
- Zhao, L., Zheng, T.Y. & Lv, G., 2013. Distinct upper mantle deformation of cratons in response to subduction: constraints from SKS wave splitting measurements in eastern China, *Gondwana Res.*, **23**, 39–53.
- Zheng, X.F., Yao, Z.X., Liang, J.H. & Zheng, J., 2010. The role played and opportunities provided by IGP DMC of China National Seismic Network in Wenchuan earthquake disaster relief and researches, *Bull. seism. Soc. Am.*, **100**(5B), 2866–2872.
- Zheng, Y., Yang, Y.Y., Ritzwoller, M., Zheng, X.F., Xiong, X. & Li, Z.N., 2010. Crustal structure of the northeastern Tibetan plateau, the Ordos block and the Sichuan basin from ambient noise tomography, *Earthq. Sci.*, **23**, 465–476.
- Zhu, L.P. & Kanamori, H., 2000. Moho depth variation in southern California from teleseismic receiver functions, *J. geophys. Res.*, **105**, 2969–2980.